Genetic analysis reveals functional redundancy and the major target genes of the *Arabidopsis* miR159 family

Robert S. Allen*†, Junyan Li*†, Melissa I. Stahle†, Aurélie Dubroué†, Frank Gubler†, and Anthony A. Millar*‡

*School of Biochemistry and Molecular Biology, Australian National University, Canberra ACT 0200, Australia; and †Commonwealth Scientific and Industrial Research Organization Plant Industry, Canberra ACT 2601, Australia

Communicated by Jim Peacock, Commonwealth Scientific and Industrial Research Organization, Canberra, Australia, August 14, 2007 (received for review June 8, 2007)

Currently, there are very few loss-of-function mutations in microRNA genes. Here, we characterize two members of the *Arabidopsis MIR159* family, miR159a and miR159b, that are predicted to regulate the expression of a family of seven transcription factors that includes the two redundant *GAMYB-like* genes, *MYB33* and *MYB65*. Using transfer DNA (T-DNA) insertional mutants, we show that a *mir159ab* double mutant has pleiotropic morphological defects, including altered growth habit, curled leaves, small siliques, and small seeds. Neither *mir159a* nor *mir159b* single mutants displayed any of these traits, indicating functional redundancy. By using reporter-gene constructs, it appears that *MIR159a* and *MIR159b* are transcribed almost exclusively in the cells in which *MYB33* is repressed, as had been previously determined by comparison of *MYB33* and *mMYB33* (an miR159-resistant allele of *MYB33*) expression patterns. Consistent with these overlapping transcriptional domains, *MYB33* and *MYB65* expression levels were elevated throughout *mir159ab* plants. By contrast, the other five *GAMYB-like* family members are transcribed predominantly in tissues where miR159a and miR159b are absent, and consequently their expression levels are not markedly elevated in *mir159ab*. Additionally, *mMYB33* transgenic plants can phenocopy the *mir159ab* phenotype, suggesting that its phenotype is explained by deregulated expression of the redundant gene pair *MYB33* and *MYB65*. This prediction was confirmed; the pleiotropic developmental defects of *mir159ab* are suppressed through the combined mutations of *MYB33* and *MYB65*, demonstrating the narrow and specific target range of miR159a and miR159b.

development | functional specificity | micro-RNA | gene regulation

Micro-RNAs (miRNAs) are 20- to 24-nucleotide (nt) small RNAs that guide the RNA-induced silencing complex in a sequence-specific manner to target mRNA(s), regulating their expression either through degradation of the transcript or translational attenuation (1). They are derived from longer noncoding RNA precursors known as primary (pri) miRNAs, being processed from these transcripts by RNase III-like enzymes known as DICER-LIKE via multiple cleavage steps (2). Their requirement for development has been well characterized. In *Arabidopsis*, miRNAs have been shown to play critical roles in stem cell formation, organ identity, leaf polarity, vascular differentiation, and cell division patterns (3). Currently, there are ≈180 known miRNA loci in *Arabidopsis*, many of which are highly conserved across the plant kingdom (3–5). For instance, the miR159 family has been found in all examined seed-bearing plants (4). In *Arabidopsis*, this family is encoded by three genes, *MIR159a*, *MIR159b*, and *MIR159c*, located in different regions of the genome (6, 7). As determined by deep sequencing, miR159a and miR159b are highly expressed compared with miR159c (5). Their mature products are 21 nt long, with miR159a and miR159b only differing in sequence at one nucleotide, whereas miR159a and miR159c differ at two nucleotides (6). These sequence differences, together with unknown expression patterns of these individual miRNAs, mean that it is uncertain whether they target similar or distinct genes.

One known target of miR159 in *Arabidopsis* is *MYB33*, which belongs to a *GAMYB-like* family of transcription factors (8). In *Arabidopsis*, there are seven members in this family, all of which share a conserved putative miR159-binding site (9). Two of these genes, *MYB33* and *MYB65*, function redundantly. This is based on strong sequence similarity, expression patterns, and genetic analysis, where only a *myb33/myb65* double mutant displays phenotypic defects (9). *MYB33* has been the focus of miR159 regulation. The isolation of miRNA-guided cleavage products for *MYB33* (10, 11) and *in planta* assays (11) have demonstrated that miR159a cleaves *MYB33* mRNA. Mutation of the miR159-binding site (without changing the amino acid sequence of the gene) within *MYB33*, generating the mutant allele known as *mMYB33* (10), resulted in dramatic expansion of the expression pattern (9). For instance, expression of the *MYB33:GUS* reporter gene construct was only detected in anthers and in seeds, whereas the *mMYB33:GUS* reporter gene has strong expression in root and shoot apices and many floral organs in addition to anthers (anther filaments, carpels, sepals, and receptacles) (9). Furthermore, transgenic *mMYB33* plants have pleiotropic developmental defects, having curled/rounded leaves, stunted growth, and altered apical dominance. In contrast, transgenic *MYB33* plants have none of these developmental defects, indicating that miRNA control of *MYB33* regulation is absolutely critical for proper plant development (9, 10). This phenotype is dramatically different than a loss-of-function *myb33/myb65* mutant (9) or plants overexpressing miR159a precursors (*35S:miR159a*), where the only observable morphological phenotype is male sterility (11, 12).

Currently, only a small number of loss-of-function mutants in miRNA genes have been reported in any organism, which is counterintuitive to the notion that their influence is widespread and that they play pivotal roles in development (13). Genetic redundancy has been proposed as a possible contributing factor to this conundrum. Here, we show that this is the case for the *Arabidopsis* miR159 family, where only a *mir159ab* double mutant exhibits pleiotropic development defects. Based on the characterization of the spatial expression pattern of the *MIR159* genes, and combined with molecular and genetic analyses, we

Author contributions: R.S.A., F.G., and A.A.M. designed research; R.S.A., J.L., M.I.S., A.D., and F.G. performed research; R.S.A., J.L., F.G., and A.A.M. analyzed data; and R.S.A., F.G., and A.A.M. wrote the paper.

The authors declare no conflict of interest.

Abbreviations: miRNA, micro-RNA; T-DNA, transfer DNA; pri, primary.

‡To whom correspondence should be addressed at: School of Biochemistry and Molecular Biology, Australian National University, Building 41, Linnaeus Way, Canberra ACT 0200, Australia. E-mail: tony.millar@anu.edu.au.

This article contains supporting information online at www.pnas.org/cgi/content/full/0707653104/DC1.

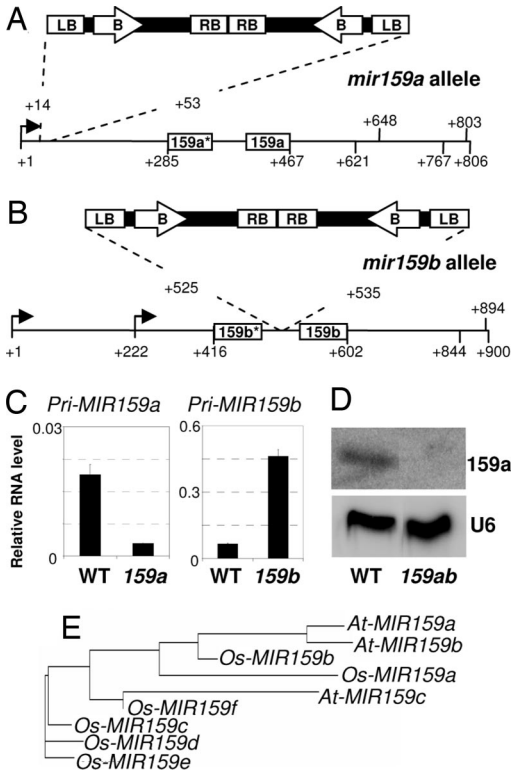

Fig. 1. Characterization and structure of the *MIR159* loci. Mapping of the pri-*MIR159* transcripts and the T-DNA insertion sites for *MIR159a* (*A*) and *MIR159b* (*B*). LB, left border; RB, right border; B, Basta-resistant gene. Arrows indicate transcriptional start sites with numbers indicating relative positions of the stem–loop regions and the varying polyadenylation sites. In both instances, the T-DNA loci were tandem inverted insertions because both plant–T-DNA junctions were isolated by using left border primers. (*C*) Relative RNA levels of pri-*MIR159* transcripts as determined by quantitative RT-PCR on RNA prepared from seedlings of wild-type, *mir159a*, and *mir159b* plants. (*D*) RNA gel blot analysis of mature miR159 levels in 72-h imbibed seeds. (*E*) A phylogenetic tree based on the stem–loop sequences of rice and *Arabidopsis MIR159* genes.

have found that the major targets of these miRNAs are even more limited in scope than previously had been predicted by using bioinformatics or overexpression strategies.

Results

Genomic Structure of the *MIR159* Genes. The primary transcripts of *MIR159a* and *MIR159b* were defined by using 5′- and 3′-end rapid amplification of cDNA ends (RACE) on RNA isolated from imbibed seeds. For *MIR159a*, a single transcriptional start site was mapped 446 bp upstream of the mature miR159a sequence, an identical position to where the transcription start-site of this gene had been previously mapped (14). In contrast, five different polyadenylation sites were found at the 3′ end from the analysis of an equal number of RACE clones (Fig. 1*A*), implying that the length of the 3′ end was highly variable. The largest transcript of *MIR159a* was 806 nt long. Similarly, variable polyadenylation sites were mapped at the 3′ end of *MIR159b*, with three different sites found from three different clones (Fig. 1*B*). Furthermore, we found two different transcription start sites, 581 and 358 nt upstream of the mature miR159b sequence. Therefore, the largest possible transcript of *MIR159b* was 900 nt long. No introns were present in either the *MIR159a* or *MIR159b* genes.

Using an RNAfold program (http://rna.tbi.univie.ac.at/cgi-bin/RNAfold.cgi) to predict the secondary structure of the various transcript forms of these two genes, we found considerable variation in their overall structures; however, in each case the stem–loop structures of the pre-miRNAs remained invariant (data not shown). This implied that each transcript isoform could be processed correctly to form a mature miRNA.

***mir159ab* Double Mutant Plants Have Pleiotropic Developmental Defects.** Searching the SIGnAL database (http://signal.salk.edu/cgi-bin/tdnaexpress), we found transfer DNA (T-DNA) insertional mutants belonging to the SAIL collection (15) that lie within *MIR159a* (SAIL_430_F11; designated here as *mir159a*) and *MIR159b* (SAIL_770_G05; designated here as *mir159b*). For *mir159a*, PCR amplification of T-DNA borders determined that the T-DNA was inserted from nucleotide +14 to +51 relative to the transcriptional start site, therefore lying within the primary transcript of the *MIR159a* gene but outside of the stem–loop structure (Fig. 1*A*). The expression of *MIR159a* had been reduced >6-fold in *mir159a* plants but not eliminated (Fig. 1*C*). Because the pre-*MIR159a* structure may still be present, this allele may only represent a hypomorphic mutation. For *mir159b*, the T-DNA has inserted within the region encoding the stem–loop structure (Fig. 1*B*), meaning that any transcript from this allele would be unable to form double-stranded RNA and be processed into a mature miRNA. It is likely that this mutation corresponds to a knockout (null) allele. We examined *MIR159b* expression in *mir159b* and found that the level of transcript containing the miRNA portion was more than seven times higher than wild type (Fig. 1*C*), suggesting that this transcript is not processed, resulting in greater stability and accumulation of this portion of the transcript. Neither *mir159a* nor *mir159b* displayed any obvious morphological traits.

A phylogenetic tree generated with the stem–loop regions of all known *Arabidopsis* and rice *MIR159* genes showed that the *Arabidopsis MIR159a* and *MIR159b* genes were highly similar, suggesting they may be functionally redundant to one another (Fig. 1*E*). In F_2 segregating plants of a cross between *mir159a* and *mir159b*, ≈1 plant in 16 (12/197; $\chi^2 = 0.09$; $P > 0.99$) had a distinctive morphological phenotype. By using PCR genotyping, these plants were confirmed to be *mir159ab* mutants, and they failed to accumulate detectable levels of mature miR159 (Fig. 1*D*). Compared with wild-type plants, *mir159ab* growth was stunted, with an altered habit including reduced apical dominance (Fig. 2*A*) and curled (hyponastic) leaves (Fig. 2*B*). Mature siliques of *mir159ab* plants were significantly shorter than those of wild type (Fig. 2*C*), indicating reduced fertility and seed set. Seeds were reduced in size and had an irregular shape (Fig. 2*D*).

***MIR159a* and *MIR159b* Have Similar Expression Patterns Consistent with *MYB33* Repression.** To determine tissue-specific expression of the individual *MIR159* genes, we performed quantitative RT-PCR with gene-specific primers against the pri-*MIR159* transcripts. *MIR159b* was expressed in mature seeds and was induced ≈20-fold after 72 h of imbibition (Fig. 3*A*). Similarly, *MIR159a* was also present in mature seeds and induced (Fig. 3*A*), but to a lesser degree (2- to 3-fold). The timing of induction corresponds to the germination of *Arabidopsis* seeds that occurs between 24 and 48 h of imbibition. *MIR159a* and *MIR159b* were also expressed in the shoot apex region and at a much higher level than *MIR159c* (Fig. 3*B*). This is consistent with *mir159ab* displaying a phenotype and suggests that no further redundancy may exist with respect to miR159-mediated processes in these tissues.

To examine the temporal and spatial expression patterns of the *MIR159* genes, we generated the reporter gene fusions *MIR159a:GUS* and *MIR159b:GUS*, where the regions immediately upstream of the miRNA stem–loop regions were fused to *GUS*. From the examination of multiple transgenic lines for each construct, we found that *MIR159a* and *MIR159b* have near-

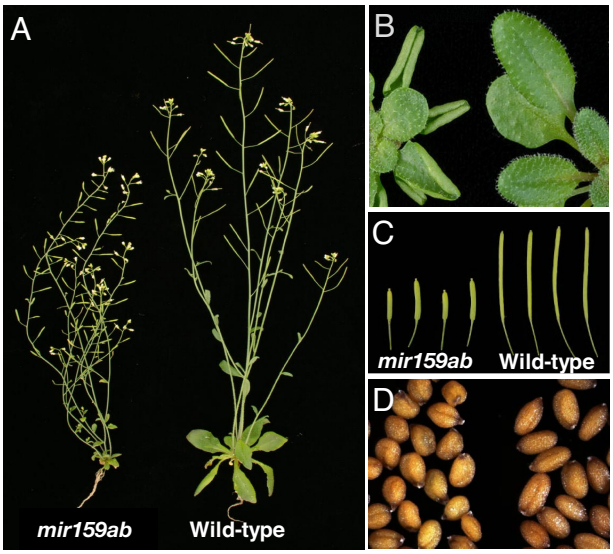

Fig. 2. Phenotypic characteristics of *mir159ab* plants. (*A*) The smaller growth stature of *mir159ab* plants. (*B*) Curled leaf phenotype (left) compared with wild-type (right). (*C*) Shorter but fatter fruits in *mir159ab* plants (left). (*D*) Smaller, irregularly shaped seeds of *mir159ab* plants (left) compared with wild type (right).

identical expression patterns (Fig. 4), a fact consistent with their redundancy. They both are strongly expressed in root tips, lateral roots, and the shoot apex region (Fig. 4 *B–D* and *F–H*), the latter possibly providing the rationale for the phenotype of *mir159ab*, because this region is where leaf primordia arise and the architecture of the plant is largely determined (16). Expression

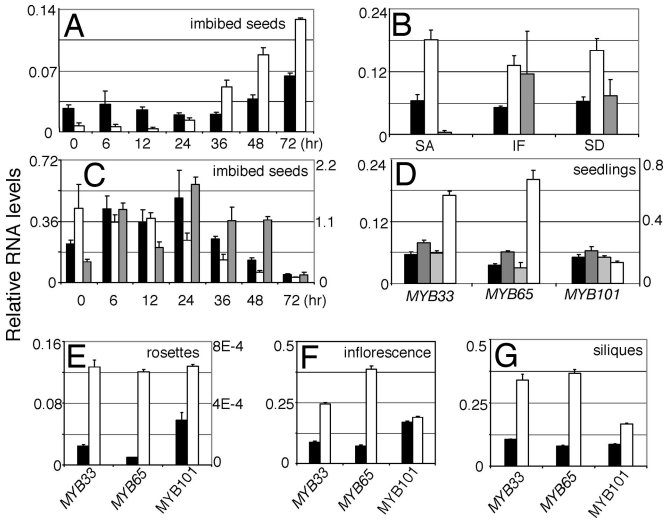

Fig. 3. RNA levels of the *MIR159* genes and their targets. (*A*) Expression of *MIR159a* (black bars) and *MIR159b* (white bars) during seed imbibition. (*B*) Expression of *MIR159a* (black bars), *MIR159b* (white bars), and *MIR159c* (gray bars) in different plant tissues. SA, shoot apical region; IF, inflorescences; SD, 3-day-old imbibed seeds. (*C*) Expression of *MYB33* (black bars), *MYB65* (white bars), and *MYB101* (gray bars) during seed imbibition. (*D*) Expression of the *GAMYB-like* genes in 3-day-old seedlings of wild type (black bars), *mir159a* (dark gray bars), *mir159b* (light gray bars), and *mir159ab* (white bars). (*E*) Expression of the *GAMYB-like* genes in wild-type (black bars) and *mir159ab* (white bars) rosettes. (*F*) Expression of the *GAMYB-like* genes in wild-type (black bars) and *mir159ab* (white bars) inflorescences. (*G*) Expression of the *GAMYB-like* genes in wild-type (black bars) and *mir159ab* (white bars) siliques. Values listed on the right side of graphs correspond to those of *MYB101*.

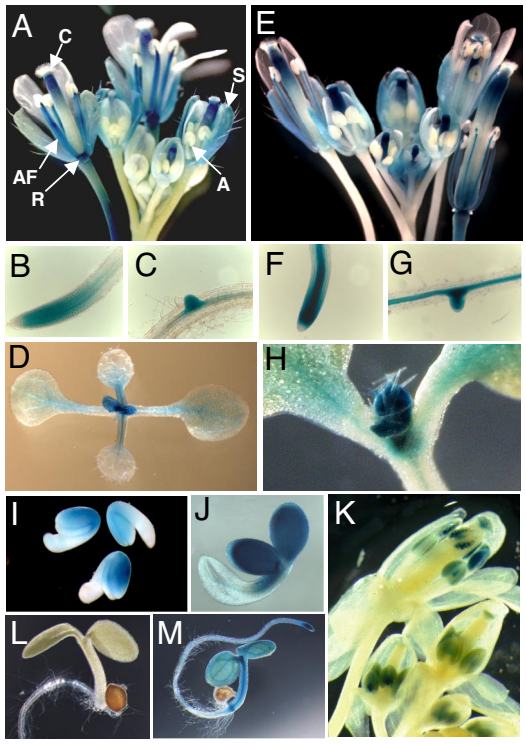

Fig. 4. Spatial expression analysis of *MIR159* and target genes. (*A–D* and *I*) GUS staining of *MIR159a:GUS* transgenic plants in inflorescence (*A*), root tips (*B*), emerging lateral roots (*C*), the shoot apex region (*D*), and seeds (*I*) imbibed for 24 h. (*E–H* and *J*) GUS staining of *MIR159b:GUS* transgenic plants in inflorescence (*E*), roots (*F*), emerging lateral roots (*G*), the shoot apex region (*H*), and 48-h-old seedlings (*J*). Staining of *MIR159b:GUS* lines was generally much stronger than that of *MIR159a:GUS* lines (*K*), *MYB101* promoter:*GUS* in inflorescences (*L*), *MYB33:GUS* in wild-type (*M*), and *MYB33:GUS* in *mir159ab*. AF, anther filament; R, receptacle; S, sepal; A, anther; C, carpels.

is seen in imbibed seeds (Fig. 4 *I* and *J*) and inflorescences (Fig. 4 *A* and *E*), receptacles, anther filaments, sepals, and carpels, with only subtle differences between *MIR159a:GUS* and *MIR159b:GUS*. Expression in these tissues coincides with the regions in which *MYB33* was repressed by miR159, as determined by the comparison of the expression patterns of *MYB33:GUS* and *mMYB33:GUS* (9). The fact that *MIR159:GUS* expression is not seen in anthers accounts for the observation that the only tissue in which *MYB33* is detected in inflorescences is the anthers (9). Therefore, throughout the plant, both *MIR159a* and *MIR159b* are expressed in a temporal and spatial pattern that is totally consistent with the pattern of miR159-mediated *MYB33* repression.

***MYB33* and *MYB65* Expression Levels Are Elevated in *mir159ab*.** We quantified the expression of the seven members of the *GAMYB-like* family that have a conserved motif that miR159 can potentially cleave (9). Of these genes, *MYB33* and *MYB65* are strongly expressed throughout the plant (12, 17). The steady-state levels of these transcripts fall during seed imbibition at the time the transcript levels of *MIR159a*/*MIR159b* increase (Fig. 3 *A* and *C*). To test whether they are under miR159 control, we measured the transcript levels of *MYB33* and *MYB65* in 3-day-old seedlings of wild-type, *mir159a*, *mir159b*, and *mir159ab* plants (Fig. 3*D*). Whereas expression was mostly unaffected in the single *mir159* mutants, in *mir159ab*, the levels of *MYB33* and *MYB65* were ≈3- and ≈5.4-fold higher than in wild type, respectively, indicating that miR159a and miR159b act redundantly in controlling the expression levels of these genes. These studies were extended to rosettes, inflores-

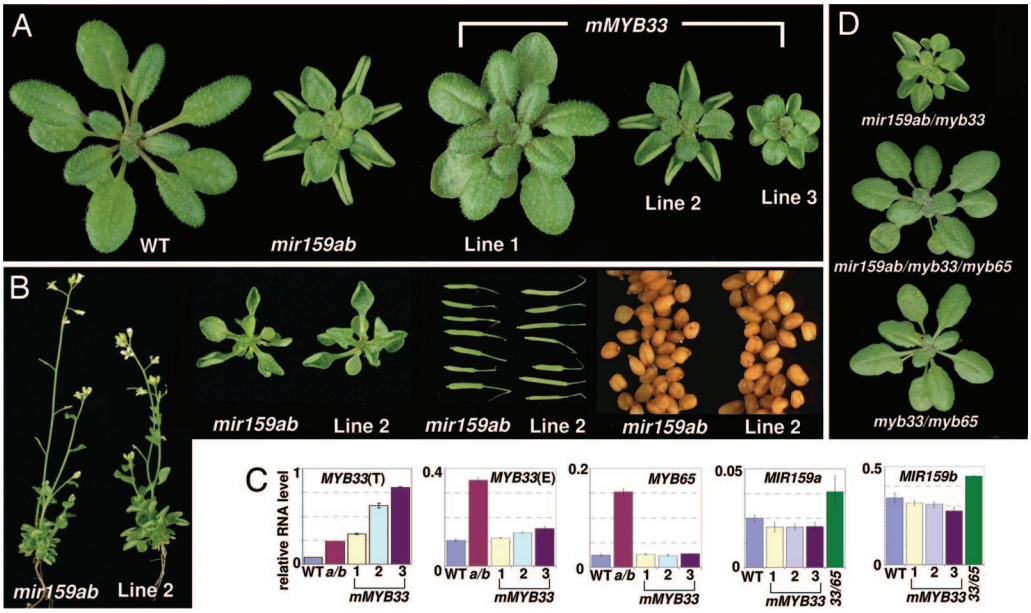

Fig. 5. Phenotypes of *mMYB33* and *mir159ab/myb33/myb65* plants. (*A*) Aerial views of rosettes of 5-week-old plants of wild-type, *mir159ab*, and three *mMYB33* lines grown under short days. (*B*) Aerial views of 3-week-old rosettes of *mir159ab* and *mMYB33* (line 2) grown under long days. Also shown are siliques, seeds, and mature plants from the same lines. (*C*) Quantitative RT-PCR of 6-week-old mature plants was used to determine the relative expression of total [(T)] *MYB33* levels, endogenous [(E)] *MYB33* (using a primer to the miR159 target site that solely amplifies the wild-type *MYB33* allele), *MYB65*, pri-*MIR159a*, and pri-*MIR159b* transcripts. (*D*) Aerial view of rosettes of *mir159ab/myb33*, *mir159ab/myb33/myb65*, and *myb33/myb65*.

cences, and siliques (Fig. 3 *E–G*). In each case, *MYB33* and *MYB65* have considerably higher transcript levels in *mir159ab* plants, demonstrating that these genes are deregulated throughout the plant. This is supported by expression of the *MYB33:GUS* transgene, which was not observable in wild-type seedlings (Fig. 4*L*) but expressed throughout *mir159ab* (Fig. 4*M*).

By contrast, *MYB101* shows little or no difference in expression levels between wild-type and *mir159ab* plants. In siliques and shoot apex regions, *MYB101* levels were only 2-fold higher. For the latter, *MYB101* transcript levels were ≈100-fold lower than *MYB33* and *MYB65*; therefore, this expression level may not be of physiological significance. In inflorescences and 3-day-old seedlings, *MYB101* levels were unchanged. In the case of the inflorescence, an *MYB101* promoter:*GUS* construct (hence without the miR159 target) only shows expression in anthers (Fig. 4*K*). This supports online Affymetrix data (www.genevestigator.ethz.ch/at/) showing that *MYB101* is overwhelmingly expressed in pollen/stamens in the inflorescence (12, 17). This implies that the vast majority of *MYB101* transcripts are not located in the same cell types as that of *MIR159a* and *MIR159b* and is a likely explanation for why *MYB101* levels are not significantly different between wild-type and *mir159ab* plants in inflorescences.

The transcript levels of the other four *GAMYB-like* family members (*MYB81*, *MYB97*, *MYB104*, and *MYB120*) are several orders of magnitude lower than *MYB33* and *MYB65* [supporting information (SI) Fig. 6]. This is consistent with online Affymetrix data, where these genes are expressed primarily in stamens/pollen, with expression either very low or insignificant in any other part of the plant (12, 17). Of the four genes, only *MYB81* has consistently higher transcript levels in *mir159ab* plants, whereas transcript levels of *MYB97* and *MYB120* were in fact lower (SI Fig. 6). In most instances, transcript level differences were only 2- to 3-fold, and this may reflect secondary effects due to the different morphologies of *mir159ab* and wild-type plants rather than miR159 regulation. However, like *MYB101*, these genes are primarily transcribed in anthers, tissues in which miR159a and miR159b appear to be absent, suggesting that they would only make minor contributions to the *mir159ab* phenotype.

***mMYB33* Plants Can Phenocopy *mir159ab*.** Previously, *mMYB33* transgenic plants (the *mMYB33* transgene being under the control of the endogenous *MYB33* promoter) were shown to have curled leaves and stunted growth (9), characteristics similar to that of *mir159ab*. For direct comparison, we grew *mir159ab* alongside three independent *mMYB33* lines that displayed a weak (line 1), intermediate (line 2), and strong (line 3) phenotype and compared their phenotypes throughout development. In all instances, the morphologies of *mir159ab* and *mMYB33* (line 2) plants appear indistinguishable from one another (Fig. 5). This includes the size and shape of the rosettes of plants grown in short days (Fig. 5*A*) or long days (Fig. 5*B*). At bolting, the size and shape of inflorescences and siliques appeared identical as did the seeds they set (Fig. 5*B*). The *MYB33* expression levels in these *mMYB33* lines were positively correlated with the severity of the phenotype (Fig. 5*C*). However, *mir159ab* did not conform to this correlation, reflecting that in addition to *MYB33*, the level of the redundant gene *MYB65* is also higher in *mir159ab* but remains unchanged in the *mMYB33* lines (Fig. 5*C*). Therefore, it is possible that total MYB33/MYB65 activity is at similar levels in *mir159ab* and *mMYB33* (line 2) plants.

We also examined the levels of *MIR159a* and *MIR159b* transcripts in the three *mMYB33* lines, because it has been hypothesized that these genes may be transcriptionally upregulated by MYB33, resulting in a regulatory feedback loop (10). However, we found no increase in *MIR159a* or *MIR159b* transcript levels in the any of the *mMYB33* lines when compared with wild-type plants (Fig. 5*C*). In addition, we failed to detect evidence of MIR159 down-regulation in the absence of MYB33 and MYB65; *MIR159* levels were not decreased in *myb33/myb65*. Finally, using a primer that discriminated between endogenous and transgenic *MYB33*, we found that the steady-state levels of endogenous *MYB33* levels were not reduced in the *mMYB33* lines (Fig. 5*C*). The fact that both endogenous *MYB33* and *MYB65* levels did not decrease in these *mMYB33* lines again supports the finding that higher miR159 levels are not present in the *mMYB33* lines.

***myb33* and *myb65* Alleles Suppress the *mir159ab* Phenotype.** All of our data point to *MYB33* and *MYB65* deregulation being predominantly responsible for the *mir159ab* phenotype. To confirm this, we crossed the *myb33* and *myb65* alleles into the *mir159ab* background. A *mir159ab*/*myb33* triple mutant displayed a milder phenotype than that of *mir159ab*, where growth was less stunted and leaf curling was less severe (Fig. 5*D*). Moreover, in a *mir159ab*/*myb33*/*myb65* quadruple mutant, all phenotypic characteristics of *mir159ab* were suppressed, and the mutant appeared to be identical to *myb33*/*myb65* (Fig. 5*D*). This reversion of the *mir159ab* traits in *mir159ab*/*myb33*/*myb65* demonstrates that *MYB33* and *MYB65* are solely responsible for the phenotype exhibited by *mir159ab* plants. Finally, because the phenotype of *mir159ab*/*myb33* reflects only deregulated *MYB65* activity, this triple mutant confirms that *MYB65* regulates similar processes to that of *MYB33* in the shoot. However, in the *mir159ab* background, *MYB33* and *MYB65* are no longer redundant; their effects have now become additive.

Discussion

Bioinformatics approaches (3), overexpression strategies (12), and isolation of miR159-cleavage products (10, 18) together predicted that the closely related *Arabidopsis MIR159* genes could regulate seven *GAMYB-like* genes. Through the characterization of *Arabidopsis* loss-of-function *mir159* mutants, along with genetic and molecular analyses, we have shown that the predominant role of miR159a and miR159b is to redundantly control just two of these genes, the redundant gene pair of *MYB33* and *MYB65*. This demonstrates a greater functional specificity than previously thought and excludes other regulatory mechanisms, such as targets with low complementarity, that exist in animals.

Currently, there are very few examples of loss-of-function mutants in plant miRNA genes, with only mutations being reported in the miR164 family (19–22). This scarcity has been thought to be due to their small size and/or potential genetic redundancy, because most miRNAs are members of small- to medium-sized gene families (3). Our findings are consistent with the latter, where the single mutants, *mir159a* and *mir159b*, failed to display a phenotype, suggesting that they are fully redundant to one another. This implies that neither *MIR159a* nor *MIR159b* are limiting in controlling target gene expression, and this was shown by the fact that neither *MYB33* nor *MYB65* expression levels increased in the *mir159a* or *mir159b* single mutants (Fig. 3*D*). Furthermore, because only the *mir159ab* double mutant displayed a phenotype under our growth conditions, this indicates that just a single copy of one wild-type allele of either *MIR159a* or *MIR159b* is sufficient to carry out miR159 function, implying that miR159 is produced in a substantial excess.

Of the seven *GAMYB-like* genes, we have demonstrated that the deregulation of the redundant gene pair of *MYB33* and *MYB65* is responsible for the *mir159ab* phenotype. There are several lines of evidence supporting this. *MIR159a:GUS* and *MIR159b:GUS* are expressed exclusively where *MYB33* was being repressed, as determined by analysis of the spatial expression patterns of *MYB33:GUS* and *mMYB33:GUS* (9). For instance, in inflorescences, the only tissue in which *MIR159a:GUS* and *MIR159b:GUS* did not overlap with *mMYB33:GUS* was in anthers, the sole tissues in which *MYB33* is expressed (9). These cotranscriptional domains of miR159a/miR159b and *MYB33* (and presumably *MYB65*) explain why *mir159ab* has global developmental defects, which is in stark contrast to transgenic plants overexpressing a *35S:miR159a* transgene that does not lead to any severe morphological defects other than in anthers (11, 12). Constitutive miR159 expression from a 35S promoter would have little impact, because the transcriptional domains of *MYB33*/*MYB65* are covered by endogenous miR159a/miR159b. Furthermore, these overlapping transcriptional domains imply that transportation of miR159a or miR159b is not required for them to repress *MYB33*, and this is in agreement with other miRNA systems where *MIRNA* transcription matched precisely to the site of its action (23, 24).

Consistent with these cotranscriptional domains, *MYB33* and *MYB65* transcript levels accumulate to 3- to 10-fold higher throughout *mir159ab* plants. In contrast, the other five *GAMYB-like* genes are predominantly transcribed in anthers and pollen, tissues in which miR159a and miR159b appear to be absent. For *MYB101*, this finding was demonstrated by the anther-specific expression of a *MYB101* promoter:GUS construct. For *MYB104*, the finding is supported by the lack of cleavage products recovered in wild-type *Arabidopsis* (10). Hence, this anther/pollen specificity would explain why the expression of these other five *GAMYB-like* genes do not dramatically increase in *mir159ab* and why *35S:miR159a* plants are male-sterile (11, 12). Furthermore, a pollen-specific gene called *DUO1* that belongs to a different class of MYB transcription factors also contains a functional miR159-binding site; when expressed as an miR159-resistant version under the constitutive 35S promoter, it produces severe developmental defects (18). However, this gene, like the five anther-specific *GAMYB-like* genes, does not contribute to the *mir159ab* phenotype; it appears that miRNA regulation is largely redundant to the transcriptional control of this gene.

The strongly overlapping expression patterns of *mMYB33:GUS* and the *MIR159:GUS* reporter genes suggest that their transcription is controlled by a common regulator, and previously it has been found that they are both induced by gibberellin (11). Furthermore, these overlapping patterns could be explained by a proposed regulatory feedback mechanism where the expression of *MYB33* induces the transcription of miR159 (11). However, the fact that the steady-state transcript levels of *MIR159a* and *MIR159b* were not elevated in the *mMYB33* transgenic lines goes against this possibility. Supporting this, endogenous *MYB33* and *MYB65* steady-state transcript levels were not lower in the *mMYB33* lines, indicating that mature miR159a/miR159b levels have remained unchanged.

By using overexpression strategies and transcriptome analysis, it has been shown that plant miRNAs appear to have only a limited number of targets that they cleave (12). Our loss-of-function strategy suggests that miR159a/miR159b predominantly regulates *MYB33* and *MYB65*, whereas the other predicted targets are predominantly transcribed in tissues where the miRNAs are absent. This scenario is similar to the few examples of miRNA mutants characterized to date. In plants, it was shown that for the *mir164abc* loss-of-function mutant, only two of the targets of miR164 were likely to account for the majority of the phenotypic changes in *mir164abc* plants (22). In animals, although *lin-4* and *let-7* are predicted to regulate many genes, either mutant can be suppressed through the mutation of single target genes (25, 26). One explanation for these observations is that the miRNAs and their targets are transcribed in adjacent but mutually exclusive expression zones, where it is thought that the role of the miRNA is to provide genetic buffering to ensure accuracy to gene-expression programs (27). Similarly, miR159a and miR159b may have a dual role in which they (*i*) cleave transcripts of *MYB33* and *MYB65* in tissues in which they are cotranscribed and (*ii*) ensure that other targets with nonoverlapping transcriptional domains are restricted to those tissues. This may explain the presence of miR159 target sites in the *GAMYB-like* genes that are apparently not targeted by miR159a or miR159b. Alternatively, the presence of these putative target sites may be required for cleavage by miR159c or the closely related miR319 family; recently, they have been shown to have activity against the *GAMYB-like* genes, although they are only very minor regulators of *MYB33* and *MYB65* (18). However, it cannot be ruled out that they are major regulators of the other five *GAMYB-like* genes. It will be of interest to examine what

selective disadvantage *mir159ab/myb33/myb65* plants have now that this highly expressed (5) and highly conserved *MIR159-MYB* regulatory component has been removed.

Materials and Methods

Determination of the pri-*MIR159* Transcripts. To determine the pri-*MIR159* transcripts, 5′ and 3′ RACE reactions were performed with first-strand cDNA synthesized on RNA isolated from imbibed seeds. A GeneRacer kit (Invitrogen Life Technologies, Carlsbad, CA) along with nested PCR primers for *MIR159a* cDNA and *MIR159b* cDNA (SI Table 1) were used to amplify the 5′ and 3′ cDNA ends. The phylogenetic tree of the stem–loop regions was constructed by using ClustalW on the program at www.ebi.ac.uk/Tools/clustalw (28).

Isolation and Genotyping of T-DNA Insertional Mutants. T-DNA mutants were found on the SIGnAL "T-DNA Express" *Arabidopsis* Gene Mapping Tool (29) and were from the Syngenta *Arabidopsis* insertion library (15). Amplification by using the following gene-specific primers (SI Table 1) detected the wild-type alleles: 159a-5 and 159b-3 gave an 884-bp fragment; 159b-5 and 159b-3 gave a 707-bp fragment. To detect the mutant T-DNA alleles, gene-specific primers were combined with the T-DNA-specific primer LB3 in the following combinations: for the *mir159a-1* allele, 159a-5 and LB3 to give a 210-bp fragment and 159b-5 and LB3 to give a 530-bp fragment.

Expression Analysis. RNA was prepared from *Arabidopsis* tissues by using a cetyltrimethylammonium bromide (CTAB) procedure (30). Total RNA (100 μg) was digested with 10 units of RQ1 RNase-free DNase (Promega, Madison, WI) for 15 min at 37°C, then cleaned by using RNeasy Plant columns (Qiagen, Valencia, CA). Five micrograms of this RNA was then used to synthesize cDNA in a 20-μl reaction using SuperScript III (Invitrogen). cDNA was diluted to 100 μl, and then 1 μl was used in 20-μl PCRs in 1× SYBR Green JumpStart Taq ReadyMix (Sigma, St. Louis, MO) and 1 μmol of each primer. Specific primers used to quantify each *Arabidopsis* gene are listed in SI Table 1, and the expression of each gene was normalized with *Cyclophilin* (At2g29960). All measurements represent the average of three replicates with error bars representing the standard error of the mean (SEM). For the *MYB* genes, two sets of primers were designed for each gene, either spanning the cleavage site or not. Differences between primer pairs were minimal, and results from only one of the pairs is shown (Fig. 3). For the *MIR159* gene, one primer was located in the stem–loop region and another was located 3′ to the stem loop. All *MIR159* primers fell within the limits of the shortest transcripts as defined in Fig. 1. Analysis of mature miR159 was carried out as described in ref. 31. Oligoprobes for miR159a and U6 were end-labeled with T4 polynucleotide kinase (Promega).

Generation of Binary Vectors and Transgenic Plants. For *pMIR159a:GUS*, upstream sequences (≈1.7 kb) of the *MIR159a* stem loop were PCR-amplified from *Arabidopsis* (Columbia) genomic DNA, with the primers mir159a-13 and mir159a-14 (SI Table 2) and cloned into the HindIII/Sal1 sites of pBI 101.1. For *pMIR159b:GUS*, upstream sequences (≈2.4 kb) of the *MIR159b* stem loop were amplified with the primers mir159b-6 and mir159b-7 and cloned into the HindIII/Xba1 sites of pB1 101.1. For *pMYB101* promoter:*GUS*, the primers 101Pro-5′ and 101Pro-3′ were used to amplify ≈2.3 kb immediately upstream of the start codon of the *MYB101* and cloned into the HindIII/Sal1 sites of pBI 101.1. All amplified DNA was sequenced and confirmed to be correct. Vectors were transformed into *Agrobacterium tumefaciens* (GV3101) and then transformed into *Arabidopsis* by using the floral dip method (32). GUS staining was performed as previously described (9).

We thank the SIGnAL Laboratory for providing the sequence-indexed *Arabidopsis* T-DNA insertion mutants (funding provided by the National Science Foundation). We thank Carl Davies for photography, M. Robertson, P. Waterhouse, D. P. Singh, and Q. Zhu for critical suggestions for the manuscript. R.S.A. was in part funded by an Emerging Science Initiative from the Commonwealth Scientific and Industrial Research Organization. M.I.S. was funded by the Pastoral Research Trust. This research was supported by Australian Research Council Grant DP0773270.

1. Bartel DP (2004) *Cell* 116:281–297.
2. Kurihara Y, Watanabe Y (2004) *Proc Natl Acad Sci USA* 101:12753–12758.
3. Jones-Rhoades MW, Bartel DP, Bartel B (2006) *Annu Rev Plant Biol* 57:19–53.
4. Axtell MJ, Bartel DP (2005) *Plant Cell* 17:1658–1673.
5. Rajagopalan R, Vaucheret H, Trejo J, Bartel DP (2006) *Genes Dev* 20:3407–3425.
6. Park W, Li J, Song R, Messing J, Chen X (2002) *Curr Biol* 12:1484–1495.
7. Rhoades MW, Reinhart BJ, Lim LP, Burge CB, Bartel B, Bartel DP (2002) *Cell* 110:513–520.
8. Woodger FJ, Millar AA, Murray F, Jacobsen JV, Gubler F (2003) *J Plant Growth Regul* 22:176–184.
9. Millar AA, Gubler F (2005) *Plant Cell* 17:705–721.
10. Palatnik JF, Allen E, Wu X, Schommer C, Schwab R, Carrington JC, Weigel D (2003) *Nature* 425:257–263.
11. Achard P, Herr A, Baulcombe DC, Harberd NP (2004) *Development (Cambridge, UK)* 131:3357–3365.
12. Schwab R, Palatnik JF, Riester M, Schommer C, Schmid M, Weigel D (2005) *Dev Cell* 8:517–527.
13. Bartel DP, Chen CZ (2004) *Nat Rev Genet* 5:396–400.
14. Xie Z, Allen E, Fahlgren N, Calamar A, Givan SA, Carrington JC (2005) *Plant Physiol* 138:2145–2154.
15. Sessions A, Burke E, Presting G, Aux G, McElver J, Patton D, Dietrich B, Ho P, Bacwaden J, Ko C, *et al.* (2002) *Plant Cell* 14:2985–2994.
16. Fletcher JC (2002) *Annu Rev Plant Biol* 53:45–66.
17. Zimmermann P, Hirsch-Hoffmann M, Hennig L, Gruissem W (2004) *Plant Physiol* 136:2621–2632.
18. Palatnik JF, Wollmann H, Schommer C, Schwab R, Boisbouvier J, Rodriguez R, Warthmann N, Allen E, Dezulian T, Huson D, *et al.* (2007) *Dev Cell* 13:115–125.
19. Baker CC, Sieber P, Wellmer F, Meyerowitz EM (2005) *Curr Biol* 15:303–315.
20. Guo HS, Xie Q, Fei JF, Chua NH (2005) *Plant Cell* 17:1376–1386.
21. Nikovics K, Blein T, Peaucelle A, Ishida T, Morin H, Aida M, Laufs P (2006) *Plant Cell* 18:2929–2945.
22. Sieber P, Wellmer F, Gheyselinck J, Riechmann JL, Meyerowitz EM (2007) *Development (Cambridge, UK)* 134:1051–1060.
23. Parizotto EA, Dunoyer P, Rahm N, Himber C, Voinnet O (2004) *Genes Dev* 18:2237–2242.
24. Alvarez JP, Pekker I, Goldshmidt A, Blum E, Amsellem Z, Eshed Y (2006) *Plant Cell* 18:1134–1151.
25. Slack FJ, Basson M, Liu Z, Ambros V, Horvitz HR, Ruvkun G (2000) *Mol Cell* 5:659–669.
26. Ambros V (1989) *Cell* 57:49–57.
27. Stark A, Brennecke J, Bushati N, Russell RB, Cohen SM (2005) *Cell* 123:1133–1146.
28. Chenna R, Sugawara H, Koike T, Lopez R, Gibson TJ, Higgins DG, Thompson JD (2003) *Nucleic Acids Res* 31:3497–3500.
29. Alonso JM, Stepanova AN, Leisse TJ, Kim CJ, Chen H, Shinn P, Stevenson DK, Zimmerman J, Barajas P, Cheuk R, *et al.* (2003) *Science* 301:653–657.
30. Chang S, Puryear J, Cairney J (1993) *Plant Mol Biol Rep* 11:113–116.
31. Fusaro AF, Matthew L, Smith NA, Curtin SJ, Dedic-Hagan J, Ellacott GA, Watson JM, Wang MB, Brosnan C, Carroll BJ, Waterhouse PM (2006) *EMBO Rep* 7:1168–1175.
32. Clough SJ, Bent AF (1998) *Plant J* 16:735–743.